

6-1-2019

Poly(ester amide) particles for controlled delivery of celecoxib.

Ian J Villamagna

Trent N Gordon

Mark B Hurtig

Frank Beier

Elizabeth R Gillies

Follow this and additional works at: <https://ir.lib.uwo.ca/chempub>



Part of the [Chemistry Commons](#)

Citation of this paper:

Villamagna, Ian J; Gordon, Trent N; Hurtig, Mark B; Beier, Frank; and Gillies, Elizabeth R, "Poly(ester amide) particles for controlled delivery of celecoxib." (2019). *Chemistry Publications*. 130.
<https://ir.lib.uwo.ca/chempub/130>

Poly(ester amide) particles for controlled delivery of celecoxib

Ian J. Villamagna,^{1,2} Trent N. Gordon,³ Mark B. Hurtig,⁴ Frank Beier,^{2,5} Elizabeth R. Gillies*^{2,3,6}

*Author to whom correspondence should be addressed: egillie@uwo.ca

¹ School of Biomedical Engineering, The University of Western Ontario, 1151 Richmond St., London, Ontario, Canada, N6A 5B9

² Bone and Joint Institute, The University of Western Ontario

³ Department of Chemical and Biochemical Engineering, The University of Western Ontario, 1151 Richmond St., London, Ontario, Canada, N6A 5B9

⁴ Ontario Veterinary College, Department of Clinical Studies, University of Guelph, 50 Stone Road, Guelph, Ontario, Canada N1G 2W1

⁵ Department of Physiology and Pharmacology, The University of Western Ontario, 1151 Richmond St., London, Ontario, Canada, N6A 3B7

⁶ Department of Chemistry, The University of Western Ontario, 1151 Richmond St., London, Ontario, Canada, N6A 5B7

ABSTRACT

Many potential pharmacological treatments for osteoarthritis (OA) can result in undesirable side effects due to the systemic administration of drugs, making the direct delivery of drugs to joints an attractive alternative. Poly(ester amide)s (PEAs) have been shown to exhibit promising properties for the development of particle-based intra-articular delivery vehicles. However, a limited range of PEA structures has been investigated. In this study, we prepared and characterized the properties of two different PEA particles composed of L-phenylalanine, sebacic acid, and either 1,4-butanediol or 1,8-octanediol (PBSe and POSe respectively). The anti-inflammatory drug celecoxib (CXB) was encapsulated into the particles. Despite minor structural differences, PBSe and POSe exhibited different thermal and mechanical properties, and encapsulation of CXB influenced these properties. PBSe-CXB particles provided a slower release of drug *in vitro* relative to POSe-CXB. Toxicity studies showed that particles without drug exhibited low toxicity to ATDC5 and C2C12 cells, while the PBSe-CXB particles exhibited concentration-dependent toxicity. Host response to the particles was evaluated in an ovine model. No adverse effects were observed following intra-articular injection and it was observed that the particles diffused into the surrounding tissues. This work shows the importance of structural tuning in PEA delivery vehicles and demonstrates their potential for further development.

Keywords: poly(ester amide), drug delivery, celecoxib, particles, intra-articular

INTRODUCTION

Osteoarthritis (OA) is a leading cause of mobility impairment and disability among adults worldwide.¹ The disease is prevalent in older generations, but the number and prevalence

continues to rise in younger populations as well.² Although there are a number of potential treatments under development, there are few clinically approved therapies. Physical therapy and lifestyle changes are often first steps in treatment,³ followed by the use of non-steroidal anti-inflammatory drugs (NSAIDs) to treat mild-to-moderate musculoskeletal pain.⁴ However, systemically administered NSAIDs suffer from poor distribution to joints and significant side effects including gastrointestinal problems and cardiovascular risks. For example, celecoxib (CXB) is an NSAID that was approved for use in OA treatment in the late 1990s.⁵ It is a potent cyclooxygenase-2 inhibitor that blocks the production of prostaglandins and attenuates the inflammatory and pain responses that are associated with OA. However, its side effects have become apparent recently, and arise in part due to the high plasma concentrations required to provide relief from OA symptoms.^{5,6} The intra-articular injection of the drug using a delivery system can potentially lead to a higher delivered dose while minimizing the side effects to off-target tissues by reducing systemic drug levels.⁷

Several different classes of drug delivery systems have been studied for intra-articular use including hydrogels,⁸ nanoparticles,^{9,10} and crystalline drug formations.¹¹ Although each of these systems has different structures and properties, they are all designed to release the drug over prolonged periods after injection into the joint without adverse reactions of the joint tissue to the delivery platform. Polymer particles are promising drug delivery systems due to their tunable properties, ease of preparation, and potential for prolonged drug release.¹² A wide variety of different polymers can be used, and the size and degradation rates of the particles can be controlled.^{13,14} Poly(ester amide)s (PEAs) are degradable polymers containing both ester and amide linkages in their backbones.^{15,16} Their thermal and mechanical properties as well as their degradation rates can be readily tuned through the incorporation of different monomers such as

amino acids, diols, and dicarboxylic acids.^{17,18} PEAs have shown favorable properties as potential drug delivery systems when formulated as micelles¹⁹ or microparticles.²⁰⁻²² They have also been shown to support the growth of cells²³⁻²⁵ and to exhibit good biocompatibility when studied *in vivo*.^{26,27} Thus far, there are very few examples involving the use of PEAs for intra-articular drug delivery. In one study, PEA particles were shown to release CXB in response to inflammation,²¹ while in another study they were demonstrated to release triamcinolone.²² In each case, the particles were shown to exhibit sustained drug release and retention in rat joints with good host response. However, there are many different structures of PEAs with different properties that remain uninvestigated to date.

We describe here the comparative study of particles composed of two different PEAs – one composed of phenylalanine, 1,4-butanediol, and sebacic acid (PBSe) and the other composed of phenylalanine, 1,8-octanediol, and sebacic acid (POSe). This simple change in the diol component leads to different properties for the two polymers. The thermal and mechanical properties of the polymers with and without CXB were studied. The drug release rates and *in vitro* toxicity studies of the particles were evaluated. In addition, host response to the PEA particles was evaluated in a large animal (ovine) model.

MATERIALS AND METHODS

General materials and procedures. PBSe and POSe were synthesized and characterized as previously reported.²⁴ Poly(vinyl alcohol) (PVA) and the 3-(4,5-dimethylthiazol-2-yl)-2,5-diphenyl tetrazolium bromide (MTT) were purchased from Millipore-Sigma (Oakville, ON). CXB was obtained from Ontario Chemicals Inc. (Guelph, ON). Dynamic light scattering was performed with a Zetasizer NanoZS from Malvern Instruments at 24.5 °C. The Z-average diameter and polydispersity index (PDI) for each type of particle were measured for three

different batches. Differential scanning calorimetry (DSC) was performed on a Q2000 from TA instruments (New Castle, DE). The heating/cooling rate was 10 °C/min from 0 to +180 °C, and the data were obtained from the second heating cycle. Statistical analyses were performed by one way ANOVA (Microsoft Excel, 2016) with alpha set at 0.05, followed by a Bonferroni post-hoc analysis, when applicable.

Tensile testing. Polymer samples, either pure or mixed with 30 wt% CXB (mixing was performed by co-dissolution of drug and polymer in CH₂Cl₂ followed by solvent evaporation), were prepared by melt pressing the polymer at 200 °C, and then cutting the resulting sheet into rectangular bars with dimensions of 25 mm × 10 mm × 1 mm (accurately measured with calipers). Tensile testing was performed on a CellScale Univert (Guelph, ON), in phosphate buffered saline (PBS) at 37 °C using a 10 N load cell. Samples were pulled at a rate of 2.5 mm/min for 240 seconds. Testing was performed in triplicate (at minimum) for each system.

Contact angle measurements. Solutions were prepared by dissolving either pure polymer or polymer with 30 wt% CXB in CH₂Cl₂ and then filtering the solution through a 0.2 µm filter. The solution was then added dropwise onto a silicon wafer until it was completely covered. The wafer was then spun at 1000 rpm for 1 min. The static water contact angles of the resulting films were then measured using 10 µL drops of deionized water with a Kruss DSA100 Drop Shape Analyzer (Hamburg, Germany). The drop was measured after 10 s of being on the surface. Three measurements were taken for each of the samples.

Preparation of particles. Particles were prepared using an oil-in-water emulsion evaporation technique. The dispersed phase of the emulsion was prepared by dissolving 400 mg of polymer in 200 mL of CH₂Cl₂. For CXB-loaded particles, 175 mg of CXB was also added to the CH₂Cl₂ phase. The continuous aqueous phase was prepared by dissolving 5 g of PVA in 1 L of deionized

water. The emulsion was made by slowly pouring the dispersed phase into the continuous phase, while stirring using a Waring Commercial immersion blender, set to low (~9000 rpm). The emulsion was mixed at 9000 rpm for an additional 2 min, then transferred to a 1 L beaker, and the organic solvent was evaporated under constant stirring overnight. Particles were collected the next day by centrifugation at 2800 g for 10 min and were then lyophilized. The dried samples were stored at 4 °C until use.

Scanning electron microscopy (SEM). SEM was performed in the University of Western Ontario's Nanofabrication Facility using a LEO 1530 instrument, operating at 2.0 kV and a working distance of 6 mm. Samples were mounted on stubs covered in carbon tape and coated with osmium using a SPI Supplies, OC-60A plasma coater. Particles in three different images and three representative sections (~30 × 30 μm) per image were measured to calculate the average diameters ± standard deviation.

Determination of drug loading and encapsulation efficiency. 10 mg of dried particles were dissolved in 1 mL of deuterated dimethyl sulfoxide and ¹H NMR spectra were obtained at 400 MHz on a Bruker 400 NMR Spectrometer (Bruker Instruments, Milton, ON). Integration values of peaks for PEA, PVA and CXB were used to calculate the percentage of each (additional details in supporting information). Drug loading (DL) and encapsulation efficiency (EE) were calculated according to equations (1) and (2).

$$\% \text{ Drug Loading} = \left(\frac{\text{Mass of drug encapsulated in particles}}{\text{Total mass of particles}} \right) \times 100 \quad (1)$$

$$\% \text{ Encapsulation Efficiency} = \left(\frac{\text{Actual CXB: PEA mass ratio}}{\text{Theoretical max. CXB: PEA mass ratio}} \right) \times 100 \quad (2)$$

In vitro release of CXB. 300 mg of particles were suspended in 5 mL of pH 7.4 phosphate buffered saline (PBS) containing 2 wt% Tween 20. The suspension was dialyzed at 37 °C using a

10 kDa molecular weight cut-off dialysis membrane against 350 mL of PBS containing 2 wt% Tween 20. Aliquots (2 mL) of the dialysate were taken daily for 20 days, and then every 5 days for up to 60 days to measure the CXB released from the particles. The amount of released drug in the dialysate was quantified using UV-visible spectroscopy at a wavelength of 253 nm based on an extinction coefficient of coefficient of $1.65 \times 10^4 \text{ L} \cdot \text{mol}^{-1} \cdot \text{cm}^{-1}$ for CXB in the same buffer system. All removed aliquots were replaced with PBS containing 2 wt% Tween 20. Furthermore, the dialysate was replaced completely when absorbance values were higher than 0.8.

***In vitro* degradation of particles in PBS.** The particles were incubated in PBS at 37 °C and were removed after 7, 14, 30 and 60 days. Once removed, the samples were washed once with deionized water then lyophilized and imaged by SEM as described above.

Cell culture. ATDC5 and C2C12 cells were thawed and cultured as previously described.^{28,29} Reagents were purchased from Sigma Aldrich (Oakville, ON). ATDC5 cells were grown in culture medium containing 225 mL of Dulbecco's Modified Eagle's Medium (DMEM) and 225 mL F12 media with the addition of 10 mL of penicillin-streptomycin (1000 units/mL), 5 mL of L-Glutamine (200 mM) and 50 mL of Fetal Bovine Serum (FBS). C2C12 cells were grown in medium comprising 500 mL of DMEM supplemented with 10 mL of penicillin-streptomycin (1000 units/ mL), 5 mL of L-Glutamine (200 mM) and 50 mL of FBS. Cells were cultured at 37 °C in an incubator with 5% CO₂. ATDC5 cells were induced to differentiate into chondrocytes with 1% Insulin-Transferrin-Selenium (ITS) in DMEM prior to experimentation.

***In vitro* toxicity.** Cells were seeded at a density of 5000 cells per well in a 96-well plate and incubated for 24 h prior to treatment. Varying concentrations of particles (0.025 -1.0 mg/mL) or free CXB (5-100 µg/mL) were suspended in cell culture media and added to the cells. Media alone was used as a negative control, and sodium dodecyl sulfate (SDS) was used as a positive

control. After 48 h, the medium was aspirated and replaced with 100 μ L of fresh medium containing 0.5 mg/mL of MTT reagent and allowed to react for 4 h in the incubator. After 4 h the plate was removed and the MTT reagent solution was aspirated. 50 μ L of dimethyl sulfoxide was added to each well to solubilize the purple crystals. The plate was then placed in a plate reader (Tecan Infinite M1000 Pro) and the absorbance at 540 nm was measured to quantify the relative metabolic activities of the cells. Four biological replicates were performed, as well as six technical replicates per plate.

***In vivo* host response.** All procedures were done in compliance with the guidelines of The Canadian Council on Animal Care guidelines (University of Guelph Protocol 3974). An ovine model was used to test the *in vivo* host response of the particles. Intra-articular injections of 50 mg of PBSe-CXB particles suspended in 1 mL of sterile saline were made into one knee (femoropatellar) joint of four sheep. Sheep were monitored daily for lameness, joint effusion, periarticular swelling, fever, and heart rate. Synovial fluid samples and plasma samples were collected under sedation at day 0, 8, and 15 days to measure leucocyte concentration using a solid state chip cytometer according to the manufacturer's instructions (Orflo Technologies, Ketchum, ID) and total protein content using a Goldberg refractometer.³⁰ Two animals were sacrificed on day 8 and two on day 15. After macroscopic assessments of the joint space, synovial membrane samples were harvested, fixed in 10% buffered formalin, and embedded in paraffin to create 5 μ M histological sections that were stained with a hematoxylin and eosin (H&E) stain.

RESULTS

Particle preparation and characterization. The PEAs PBSe and POSe (Figure 1) were synthesized as previously reported and were characterized by ^1H NMR spectroscopy, size exclusion chromatography, and DSC (Figures S1-S5).²⁴ The batch of PBSe used in the current work had a number average molar mass (M_n) of 30 kg/mol and dispersity (D) of 2.0 while POSe had an M_n of 18 kg/mol and a $D = 1.9$. PBSe had a glass transition temperature (T_g) of 34 °C, while POSe had a T_g of 14 °C and a melting temperatures (T_m) of 106 and 150 °C. Using these PEAs, four different types of particles were prepared: non-drug-loaded PBSe (PBSe-NDL), non-drug-loaded POSe (POSe-NDL), CXB-loaded PBSe (PBSe-CXB) and CXB-loaded POSe (POSe-CXB). The average particle size was determined using the SEM and DLS (Figure 2, Table 1). Based on DLS, PBSe-NDL had a Z-average diameter of 790 ± 64 nm, which was not statistically significantly different from PBSe-CXB with a Z-average diameter of 836 ± 51 nm ($p = 0.56$). In contrast, both POSe-NDL and POSe-CXB were smaller with Z-average diameters of 487 ± 10 nm and 398 ± 13 nm, respectively, and were statistically significantly different from one another ($p = 0.02$). SEM confirmed that the particles were all spherical. The diameters measured by SEM were generally larger than those obtained by DLS, but the trends were similar, with both POSe-based particles being statistically smaller than their PBSe counterparts ($p = 0.03$). Based on SEM, neither PBSe or POSe exhibited a significant change in diameter when loaded with CXB ($p = 0.09$). The drug loading was 23 wt% for PBSe particles, and 20% for POSe, with encapsulation efficiencies of 84 and 69%, respectively.

DSC was used to investigate the effects of 30 wt% CXB incorporation on the thermal properties of the bulk polymers (Figure S5). For PBSe, incorporation of CXB resulted in glass transitions at 31 and 45 °C, while for POSe it resulted in disappearance of crystallinity and an increase in the T_g to 29 °C. DSC was also performed on the particles (Figure 3). PBSe-NDL had

a T_g of 38 °C while POSe-NDL had a T_g of 30 °C. The addition of CXB to the particles resulted in a small increase in T_g for PBSe-CXB to 41 °C, but no change for POSe-CXB. No melting point for CXB was observed.

Tensile testing of PBSe and POSe as well as their blends with and without 30 wt% CXB was performed in water at 37 °C. POSe had the highest Young's modulus of 26 ± 16 MPa, while PBSe had a modulus of 1.17 ± 0.19 MPa (Table 2). The addition of CXB to the polymers decreased the Young's moduli to 0.43 ± 0.15 MPa and 0.83 ± 0.68 MPa for POSe-CXB and PBSe-CXB, respectively.

Contact angle measurements were performed to compare the hydrophobicities of the polymers and their blends with CXB in the form of thin films (Table 2). PBSe was more hydrophilic, having a contact angle of 77.4 ± 0.9 °, compared to POSe having a contact angle of 85.3 ± 1.7 °. The incorporation of CXB significantly increased the hydrophilicity in each case, lowering the contact angle to 72.3 ± 0.8 ° for PBSe-CXB and 79.2 ± 0.1 ° for POSe-CXB.

***In vitro* release of CXB and particle degradation.** The release of CXB from PBSe-CXB and POSe-CXB particles was determined through dialysis and detection of the CXB in the dialysate. Both particle systems exhibited a slower release than free CXB, which was used as a control (Figure 4). PBSe-CXB had a slower release than POSe-CXB. At 40 days, 25% of the loaded CXB had been released from PBSe-CXB, while 70% had already been released from the POSe-CXB. The degradation of particles in pH 7.4 PBS at 37 °C over time was probed by SEM. PBSe-CXB particles showed a distinct surface degradation at all time points, with increased degradation over time (Figure 5A-C). However, particles were still visible at day 60. POSe-CXB underwent more rapid degradation, with the loss of most particles apparent by 7 and 14 days (Figure 5D-E).

In vitro and in vivo studies. Based on their CXB release and degradation properties, PBSe particles were evaluated using MTT assays in two different cell lines – mouse cartilage-like ATDC5 cells and mouse myoblasts C2C12. After 48 h of incubation with PBSe-NDL particles both cell lines retained high metabolic activity at all concentrations evaluated, up to 1 mg/mL (Figure 6), as measured by MTT activity. In contrast, PBSe-CXB particles exhibited concentration dependent decreases in metabolic activity for both cell lines, with a 50% reduction at ~0.1 mg/mL. Free CXB also exhibited concentration-dependent toxicity with a 50% reduction in metabolic activity of ATDC5 and C2C12 cells at ~20 µg/mL and 40 µg/mL, respectively (Figures S8-S9).

After intra-articular injections of PBSe-CXB (50 mg particles in 1 mL of saline) in sheep, there was minimal effusion for 48 hours, but no lameness, fever, changes in eating habits, or changes in social interactions were observed. Synovial fluid analysis showed a small but significant increase in both white blood cells (WBC) and total protein concentrations post injection (Figure 7). Histological analysis showed mild synovial intimal hyperplasia, with some increase in vascularity but no cellular infiltration. Specifically, the particles could be identified in the synovial lining and subintimal layer, but there was no cellular response (Figure 8).

DISCUSSION

A wide variety of PEAs having different structures and properties have been previously reported.^{15,16} For the current work, PBSe and POSe were selected as they are easily synthesized, and have shown promising biological properties such as high cell compatibility in previous work.^{23,24} In addition, despite the minor structural difference of containing butyl versus octyl chains in their backbones, they have been shown to exhibit different thermal and mechanical

properties.³¹ The T_g value of 34 °C for the bulk PBSe used in the current work was similar to those previously reported for this polymer (38 – 40 °C).^{24, 31} POSe was semicrystalline in the bulk state with T_m values of 106 and 150 °C similar to those previously reported.^{24, 31} However, the T_g of 14 °C measured for POSe was significantly lower than that previously reported (22 – 28 °C), which can likely be attributed to its lower molar mass (M_n of 18 kg/mol for current versus 30 – 78 kg/mol previously).

CH_2Cl_2 was selected as the organic solvent for the emulsification-evaporation particle preparation because it is a good solvent for both PEA and CXB and is immiscible with water, as required for the process. In contrast to previously reported work on PEA particles, the use of CH_2Cl_2 did not lead to particles of irregular shape.²⁰ This may result from different parameters such as solvent ratios, mixing time and evaporation time used in the current work.³² We fixed the PEA concentration at 2 mg/mL because of solubility limitations. In addition, we fixed the water: CH_2Cl_2 at 5:1 mL based on previous work.²⁰ Different emulsification processes were explored and an immersion blender operating at 9000 rpm proved to be the best, whereas a magnetic stir bar led to large conglomerates of material in addition to spherical particles and sonication appeared to result in breakdown of particles. 5 wt% PVA in the water was the most appropriate concentration as lower concentrations led to insufficient particle stabilization and consequent agglomeration, whereas higher concentrations led to particles that were immersed in a large excess of PVA and were difficult to purify.

It has been suggested that particles of different sizes have different advantages and limitations in the context of intra-articular drug delivery. The size of synthesized particles was consistent with what is believed to be suitable for intra-articular delivery. With a diameter of 500-1000 nm, it is expected that particles will be small enough to not induce a significant immune response, but

large enough to have a long residence time in the joint, and not be rapidly cleared.³³ The diameters measured by DLS were consistently smaller than those measured by SEM across all samples. While larger particles are often emphasized in DLS measurements due to their increased scattering of light relative to smaller particles, in this case it is likely that the larger particles settled during the measurement and were thus not completely captured in the size distribution. POSe particles were significantly smaller than the PBSe particles in both their CXB-loaded and non-loaded forms. However, a small fraction of larger (>1000 nm) particles was detected for POSe-NDL by both DLS and SEM. As supported by the contact angle measurements, POSe is more hydrophobic, owing to the increased length of the diol component. This may make these particles more difficult to disperse, while at the same time favoring interactions with the PVA surfactant, which may lead to the stabilization of smaller particles. It was also notable that the incorporation of CXB produced particles with higher purity (less surrounding material) in the case of both POSe-CXB and PBSe-CXB. As previously reported, it was expected that the CXB could play the role of a surfactant, which could further stabilize the emulsion and allow for morphologically-optimized particles.³⁴

High drug loading contents and acceptable encapsulation efficiencies were achieved for both the PBSe and POSe particles. High hydrophobicity of CXB results in its preferential partition into the organic phase, thereby resulting in its encapsulation rather than loss into the aqueous phase. The high drug content achievable also suggests high compatibility of CXB with the PEAs used here. It is notable that the drug content of our particles was much higher than the 5 wt% CXB reported by Janssen et. al in different PEA particles.²¹ Higher drug content is desirable to minimize the dose of polymer required to administer a given quantity of drug.

In comparing the thermal properties of the bulk polymers to those of the particles both with and without CXB, PBSe-NDL particles had a slightly higher T_g of 38 °C compared to 34 °C for the bulk polymer. A secondary T_g was observed at 60-70 °C for all of the particles, which likely corresponds to the PVA coating the particles and it is possible that some incorporation of PVA into the particles modestly increased the T_g . The incorporation of CXB into the PBSe particles increased the T_g by 3 °C, suggesting that interactions between CXB and PBSe decreased the mobility of the polymer. The incorporation of CXB into bulk PBSe resulted in a main T_g value of 31 and a small secondary T_g of 45 °C, suggesting the presence of small CXB-rich domains due to some degree of phase separation. This phase separation may have been induced by the melt pressing process, but it was deemed important to process the samples in the same way as for the tensile testing samples in order to correlate their properties. While POSe in the bulk state was semicrystalline, no T_m was observed for POSe particles and instead a single T_g value of 30 °C was observed. This result highlights the importance of the processing conditions on the properties of the polymers. While the incorporation of CXB into the POSe particles did not affect their T_g , the incorporation of CXB into bulk POSe resulted in complete loss of crystallinity and a single T_g value of 29 °C, a result that is important for understanding the tensile properties of the samples. The thermal properties of bulk POSe-CXB were consequently very similar to POSe-CXB particles. No melting point for CXB was observed in the expected range (157-159 °C) for any of the particles, suggesting that CXB was mixed well with the PEAs.

The Young's moduli and ultimate tensile strengths of melt pressed polymers and their blends with CXB were explored. These tests were performed with the samples in a hydrated state at 37 °C to mimic physiological conditions, particularly because water is known to have a significant plasticizing effect on amorphous polymers.³⁵ Indeed, increasing the temperature to 37 °C

immersed in water relative to ambient temperature in the dry state lowered the Young's modulus of PBSe from ~ 1 GPa to 1.17 ± 0.19 MPa.³¹ The addition of CXB resulted in a further decrease in modulus to 0.83 ± 0.68 MPa. The decrease may correlate with the observed lowering of the main T_g for bulk PBSe-CXB relative to PBSe. Consistent with a decreased water contact angle upon CXB incorporation, it may also be attributed to CXB's ability to hydrogen bond to water, thereby enhancing interactions of the blends with water, further increasing the water plasticization effect. This brings the modulus into a range similar to articular cartilage,³⁶ which is desirable as the injection of high modulus materials into the joint may be expected to cause irritation. Similar trends were observed for the ultimate tensile strength, with immersion in water resulting in a ~ 30 -fold decrease relative to the polymer in the dry state at ambient temperature and CXB inducing a further decrease.³¹ POSe-NDL had a higher Young's modulus and higher tensile strength in water at 37°C , which likely arises from its semi-crystallinity in the bulk, and would not likely be reflective of the properties of the particles, which were not semicrystalline. However, upon incorporation of CXB, POSe-CXB became completely amorphous, resulting in a decrease in the Young's modulus to a value lower than that of PBSe-CXB. Plasticization by water may play an additional role in decreasing the modulus as a decrease in water contact angle was also observed for POSe upon CXB incorporation. The mechanical properties of the bulk POSe-CXB should reflect those of the POSe-CXB particles as they had very similar thermal properties. Overall, these results highlight the importance of small PEA structural variations as well as processing conditions in controlling the properties of the polymers under different conditions.

Due to CXB's very low solubility in water, 2 wt% of the surfactant Tween 20 was added to the dialysis release medium. A control experiment performed by the addition of unencapsulated

solid CXB into a dialysis bag showed that CXB dissolution and diffusion through the dialysis bag was still quite slow with ~50% release after 10 days. However, it was faster than for CXB loaded into PEA particles, confirming that particle encapsulation was able to provide sustained release of drug due to rate-limiting release from the particles. PBSe-CXB in particular showed very slow release of drug, with only 36% released over 60 days. SEM images of the particles after 14, 30, and 60 days in PBS at 37 °C supported that the slow release can likely be attributed to slow degradation of the particles. The lack of burst release and ability of the PBSe particles to retain the drug over a prolonged time period are favorable properties for an intra-articular delivery system as it is desirable to maximize the time between required doses. On the other hand, POSe-CXB exhibited a release rate of CXB that approached that of the free drug and SEM images showed a rapid loss of particle structure even after 7-14 days. We attribute this behavior to the low T_g of POSe-CXB in water, which may result in particle fusion and reorganization, processes which are accompanied by the loss of CXB. It is also possible that the lower molar mass of POSe compared to PBSe resulted in more rapid polymer degradation.

PBSe particles were selected for biological studies due to their favorable CXB release and degradation properties. Cytotoxicity studies were performed on ATDC5 “chondrocyte-like” cells and C2C12 myoblast cells. The use of two different cell lines allows for the detection of cell line-dependent responses to the particles, and should provide an indication of how different tissues might react to the particles. C2C12 was selected as it is a commonly used cell line for *in vitro* work. High metabolic activities were retained for the PBSe-NDL particles in both cell lines at concentrations up to 1 mg/mL. This was expected as previous studies have shown that PBSe was well tolerated by cells.^{23,24} On the other hand, concentration-dependent toxicity was observed for PBSe-CXB in both cell lines. This was expected as we observed significant toxicity

of free CXB on both cell lines at 20 – 40 µg/mL and PBSe-CXB particles can release CXB during the assay. It is also in agreement with previous studies, where CXB has been showed to exhibit toxicity *in vitro*.³⁷

In vivo pilot studies were performed in an ovine model. This large animal model allowed for a robust histological examination, and serial synovial fluid analysis. Intra-articular injections were performed on 4 sheep, which was sufficient to provide an initial indication of host response to the PBSe-CXB particles. A dose of 50 mg/animal was selected in order to have the most possible CXB injected into the joint, while maintaining the injectability of the drug delivery system. As reported by Janssen et al. for different PEA particles, PBSe-CXB particles appeared to have been engulfed by synovial lining cells and local macrophages, resulting in particles within the synovial villi.²¹ The mild increase in vascularity and intimal lining cells is consistent with the trauma of synovial fluid collection. The particles themselves appeared to be remarkably inert. White blood cell and protein concentrations in the synovial fluid post injection did increase significantly, but the increase was small and within the levels expected from arthrocentesis alone. Overall, our observations were similar to those reported previously following the injection of a CXB-containing hydrogel into horse joints.³⁸

CONCLUSIONS

Particles composed of two different PEAs were prepared and characterized. It was found that small structural differences in the polymers led to significant changes in the particle properties including their T_g values and Young's moduli and also led to different CXB release rates. The slower release profile of the PBSe-CXB particles makes them more ideal for intra-articular drug delivery. PBSe-NDL particles were found to be well tolerated by both ATDC5 and C2C12 cells, while the presence of CXB in the PBSe-CXB particles induced concentration-dependent toxicity

in both cells lines. Initial *in vivo* results in an ovine model showed that the PBSe particles migrated to the synovial membrane and surrounding tissue and were well tolerated at a dose of 50 mg/animal.

Acknowledgements

We thank Tristan Harrison for help with the contact angle measurements. We thank the Natural Sciences and Engineering Research Council of Canada (NSERC) CONNECT CREATE Training Grant for funding IJV and the University of Guelph Equine Research program (EG 2016-04) and NSERC (DG 2016-04636 to ERG) for funding the work. FB thanks The Arthritis Society for funding of this project and is the recipient of a Canada Research Chair Award.

References

1. Neogi T. The epidemiology and impact of pain in osteoarthritis. *Osteoarthr Cartil* 2013;21:1145-1153.
2. Whittaker JL, Woodhouse LJ, Nettel-Aguirre A, Emery CA. Outcomes associated with early post-traumatic osteoarthritis and other negative health consequences 3-10 years following knee joint injury in youth sport. *Osteoarthr Cartil* 2015;23:1122-9.
3. Vincent HK, Heywood K, Connelly J, Hurley RW. Obesity and weight loss in the treatment and prevention of osteoarthritis. *PM R* 2012;4:S59-S67.
4. Cheng DS, Visco CJ. Pharmaceutical therapy for osteoarthritis. *PM R* 2012;4:S82-S8.
5. Puljak L, Marin A, Vrdoljak D, Markotic F, Utrobicic A, Tugwell P. Celecoxib for osteoarthritis. *Cochrane Database Syst Rev*; 2017; Art. No.: CD009865.
6. Simon LS, Weaver AL, Graham DY, Kivitz AJ, Lipsky PE, Hubbard RC, Isakson PC, Verburg KM, Yu SS, Zhao WW, Geiss GS. Anti-inflammatory and upper gastrointestinal effects of celecoxib in rheumatoid arthritis: A randomized controlled trial. *JAMA* 1999;282:1921-1928.

7. Maudens P, Jordan O, Allemann E. Recent advances in intra-articular drug delivery systems for osteoarthritis therapy. *Drug Discov Today* 2018; <https://doi.org/10.1016/j.drudis.2018.05.023>
8. He Z, Wang B, Hu C, Zhao J. An overview of hydrogel-based intra-articular drug delivery for the treatment of osteoarthritis. *Colloids Surf., B* 2017;154:33-39.
9. Kang ML, Ko JY, Kim JE, Im GI. Intra-articular delivery of kartogenin-conjugated chitosan nano/microparticles for cartilage regeneration. *Biomaterials* 2014;35:9984-9994.
10. Kim SR, Ho MJ, Kim SH, Cho HR, Kim HS, Choi YS, Choi YW, Kang MJ. Increased localized delivery of piroxicam by cationic nanoparticles after intra-articular injection. *Drug Des Devel Ther* 2016;10:3779-3787.
11. Rovati LC, Girolami F, Persiani S. Crystalline glucosamine sulfate in the management of knee osteoarthritis: Efficacy, safety, and pharmacokinetic properties. *Ther Adv Musculoskelet Dis* 2012;4:167-180.
12. Freiberg S, Zhu XX. Polymer microspheres for controlled drug release. *Int J Pharm* 2004;282:1-18.
13. Saralidze K, Koole LH, Knetsch MLW. Polymeric microspheres for medical applications. *Materials* 2010;3:3537-3564.
14. Tran VT, Benoit JP, Venier-Julienne MC. Why and how to prepare biodegradable, monodispersed, polymeric microparticles in the field of pharmacy? *Int J Pharm* 2011;407:1-11.
15. Fonseca AC, Gil MH, Simões PN. Biodegradable poly(ester amide)s – a remarkable opportunity for the biomedical area: Review on the synthesis, characterization and applications. *Prog Polym Sci* 2014;39:1291-1311.

16. Diaz A, Katsarava R, Puiggali J. Synthesis, properties and applications of biodegradable polymers derived from diols and dicarboxylic acids: From polyesters to poly(ester amide)s. *Int J Mol Sci* 2014;15:7064-123.
17. Pang X, Chu CC. Synthesis, characterization and biodegradation of functionalized amino acid-based poly(ester amide)s. *Biomaterials* 2010;31:3745-3754.
18. Rodriguez-Galan A., Franco L., Puiggali J. Degradable Poly(ester amide)s for Biomedical Applications. *Polymers* 2011;3:65-99.
19. Zilinskas GJ, Soleimani A, Gillies ER. Poly(ester amide)-poly(ethylene oxide) graft copolymers: Towards micellar drug delivery vehicles. *Int J Polym Sci* 2012;2012:1-11.
20. Guo K, Chu CC. Biodegradable and injectable paclitaxel-loaded poly(ester amide)s microspheres: Fabrication and characterization. *J Biomed Mater Res, Part B* 2009;89:491-500.
21. Janssen M, Timur UT, Woike N, Welting TJ, Draaisma G, Gijbels M, van Rhijn LW, Mihov G, Thies J, Emans PJ. Celecoxib-loaded pea microspheres as an auto regulatory drug-delivery system after intra-articular injection. *J Controlled Release* 2016;244:30-40.
22. Rudnik-Jansen I, Colen S, Berard J, Plomp S, Que I, van Rijen M, Woike N, Egas A, van Osch G, van Maarseveen E, Messier K, Chan A, Thies J, Creemers L. Prolonged inhibition of inflammation in osteoarthritis by triamcinolone acetonide released from a polyester amide microsphere platform. *J Controlled Release* 2017;253:64-72.
23. Knight DK, Gillies ER, Mequanint K. Biomimetic L-aspartic acid-derived functional poly(ester amide)s for vascular tissue engineering. *Acta Biomater* 2014;10:3484-3496.

24. Knight DK, Gillies ER, Mequanint K. Strategies in functional poly(ester amide) syntheses to study human coronary artery smooth muscle cell interactions. *Biomacromolecules* 2011;12:2475-2487.
25. Yamanouchi D, Wu J, Lazar AN, Kent KC, Chu CC, Liu B. Biodegradable arginine-based poly(ester-amide)s as non-viral gene delivery reagents. *Biomaterials* 2008;29:3269-3277.
26. Peters T, Kim SW, Castro V, Stingl K, Strasser T, Bolz S, Schraermeyer U, Mihov G, Zong M, Andres-Guerrero V and others. Evaluation of polyesteramide (PEA) and polyester (PLGA) microspheres as intravitreal drug delivery systems in albino rats. *Biomaterials* 2017;124:157-168.
27. Lips PA, van Luyn MJ, Chiellini F, Brouwer LA, Velthoen IW, Dijkstra PJ, Feijen J. Biocompatibility and degradation of aliphatic segmented poly(ester amide)s: In vitro and in vivo evaluation. *J Biomed Mater Res, Part A* 2006;76:699-710.
28. Wang G, Woods A, Sabari S, Pagnotta L, Stanton L-A, Beier F. RhoA/ROCK signaling suppresses hypertrophic chondrocyte differentiation. *J Biol Chem* 2004;279:13205-13214.
29. McMahon DK, Anderson PA, Nassar R, Bunting JB, Saba Z, Oakeley AE, Malouf NN. C2C12 cells: Biophysical, biochemical, and immunocytochemical properties. *Am J Physiol* 1994;266:C1795-C1802.
30. George JW, O'Neill SL. Comparison of refractometer and biuret methods for total protein measurement in body cavity fluids. *Vet Clin Pathol* 2001;30:16-18.

31. Soleimani A, Drappel S, Carlini R, Goredema A, Gillies ER. Structure–property relationships for a series of poly(ester amide)s containing amino acids. *Ind Eng Chem Res* 2014;53:1452-1460.
32. Nihnat N, Schugens C, Grandfils C, Jerome R, Teyssie P. Polylactide microparticles prepared by double emulsion/evaporation technique. *Pharm Res* 1994;11:1479-1484.
33. Edwards SH. Intra-articular drug delivery: The challenge to extend drug residence time within the joint. *Vet J* 2011;190:15-21.
34. Sekhon BS. Surfactants: Pharmaceutical and medicinal aspects. *J Pharm Technol Res Manag* 2013;1:43-68.
35. Hancock BC, Zografi G. The relationship between the glass transition temperature and the water content of amorphous pharmaceutical solids. *Pharm Res* 1994;11:471-477.
36. Camarero-Espinosa S, Rothen-Rutishauser B, Foster EJ, Weder C. Articular cartilage: From formation to tissue engineering. *Biomater Sci* 2016;4:734-767.
37. Amrite AC, Ayalasomayajula SP, Cheruvu NP, Kompella UB. Single periocular injection of celecoxib-PLGA microparticles inhibits diabetes-induced elevations in retinal PGE₂, VEGF, and vascular leakage. *Invest Ophthalmol Vis Sci* 2006;47:1149-1160.
38. Petit A, Redout EM, van de Lest CH, de Grauw JC, Muller B, Meyboom R, van Midwoud P, Vermonden T, Hennink WE, Rene van Weeren P. Sustained intra-articular release of celecoxib from in situ forming gels made of acetyl-capped PCLA-PEG-PCLA triblock copolymers in horses. *Biomaterials* 2015;53:426-36.

FIGURE LEGENDS

Figure 1. Chemical structures of the polymers PBSe and POSe.

Figure 2. A) DLS diameter distributions by volume % for CXB and non-drug-loaded particles made from either PBSe or POSe; B-E) SEM micrographs of prepared particles showing their spherical structures and size distributions: B) PBSe-NDL; C) PBSe-CXB; D) POSe-NDL; E) POSe-CXB. Material surrounding the particles in B and D is likely PVA.

Figure 3. DSC thermograms of the drug-loaded and non-drug-loaded particles showing that the T_g was increased through CXB incorporation only for PBSe. A subtle transition corresponding to PVA was observed at 60 – 70 °C but no melting temperature was observed for CXB.

Figure 4. CXB release from PBSe-CXB particles and POSe-CXB particles in pH 7.4 PBS containing 2 wt% Tween 20 showing slower release of CXB from the PBSe-CXB particles. The release of insoluble free CXB through the dialysis membrane was also measured as a control to show that the release rate was not limited by the drug dissolution rate.

Figure 5. Degradation of PEA particles in pH 7.4 PBS at 37 °C: A-C) PBSe-CXB particles after A) 14, B) 30 and C) 60 days; D-E) POSe-CXB particles after D) 7 and E) 14 days. All images were obtained at the same magnification. While particles were still observed for PBSE-CXB at 60 days, most of the POSe-CXB particles were rapidly eroded.

Figure 6. Metabolic activity of A) ATDC5 cells and B) C2C12 cells as measured by an MTT assay after a 48 h incubation with PBSe-CXB or PBSe-NDL particles (N = 4).

Figure 7. Synovial fluid analysis of injected sheep joints: A) Protein levels in synovial fluid at days 0, 8 and 15. * Indicates a significant difference between day 0 and day 8. (ANOVA $p = 0.04$) B) WBC levels at days 0, 8 and 15. * Indicates a statistically significant difference between day 0 and day 8 (ANOVA $p = 0.0001$). $N = 4$ at days 0 and 8 and $N = 2$ at day 15.

Figure 8. Immunohistochemical analysis of the synovial membrane of an injected sheep 15 days post injection. Hematoxylin and eosin staining was performed on sections of sheep synovium. Particles are visible within the membrane (indicated with red arrows).

Table 1. Average diameters of the PEA-based particles obtained by DLS and SEM and CXB loading and encapsulation efficiency measured by NMR spectroscopy.

Particle Composition	Z-Average diameter (DLS) (nM)	Measured particle diameter (SEM) (nM)	CXB loading (wt%)	CXB encapsulation efficiency (%)
PBSe-NDL	790 ± 64	870 ± 74	-	-
PBSe-CXB	836 ± 51	1040 ± 100	23 ± 1	84 ± 4
POSe-NDL	487 ± 10	867 ± 92	-	-
POSe-CXB	398 ± 13	637 ± 101	20 ± 4	69 ± 15

Table 2. Young's modulus and ultimate tensile strengths of the polymers and their blends with CXB, as measured by tensile testing in water at 37 °C and contact angles of polymer films.

Errors on the measurements correspond to the standard deviations.

Polymer Composition	Young's modulus (MPa)	Ultimate Tensile Strength (MPa)	Contact angle (°)
PBSe-NDL	1.17 ± 0.19	0.66 ± 0.3	77.4 ± 0.9
PBSe-CXB	0.83 ± 0.68	0.04 ± 0.01	72.3 ± 0.8
POSe-NDL	26 ± 16	5.6 ± 2.2	85.3 ± 1.7
POSe-CXB	0.43 ± 0.15	0.16 ± 0.04	79.2 ± 0.1

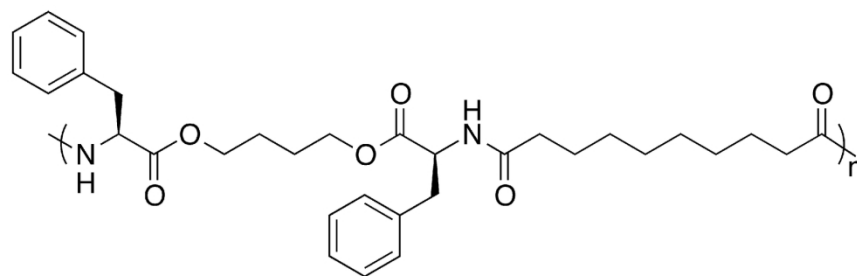
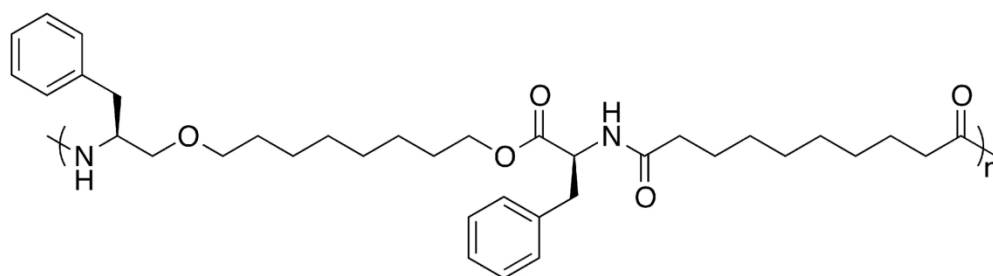
**PBSe****POSe**

Figure 1. Chemical structures of the polymers PBSe and POSe.

85x59mm (600 x 600 DPI)

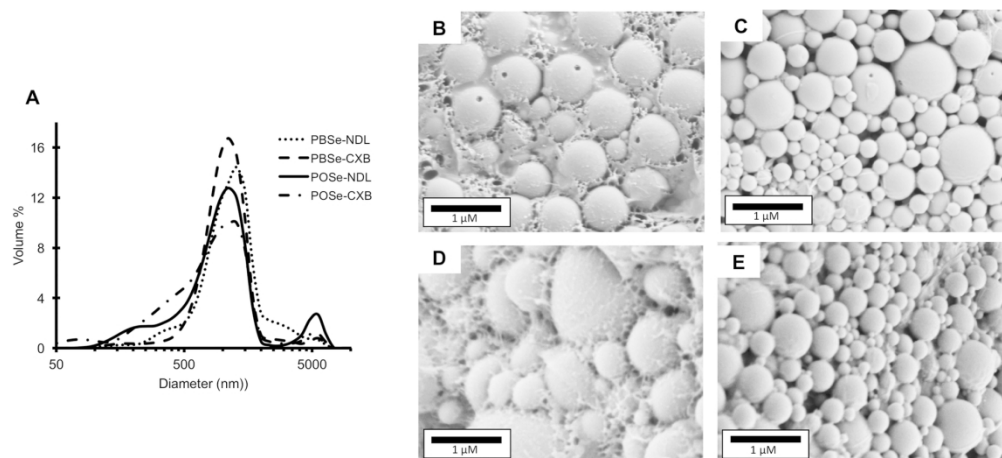


Figure 2. A) DLS diameter distributions by volume % for CXB and non-drug-loaded particles made from either PBSe or POSe; B-E) SEM micrographs of prepared particles showing their spherical structures and size distributions: B) PBSe-NDL; C) PBSe-CXB; D) POSe-NDL; E) POSe-CXB. Material surrounding the particles in B and D is likely PVA.

165x75mm (300 x 300 DPI)

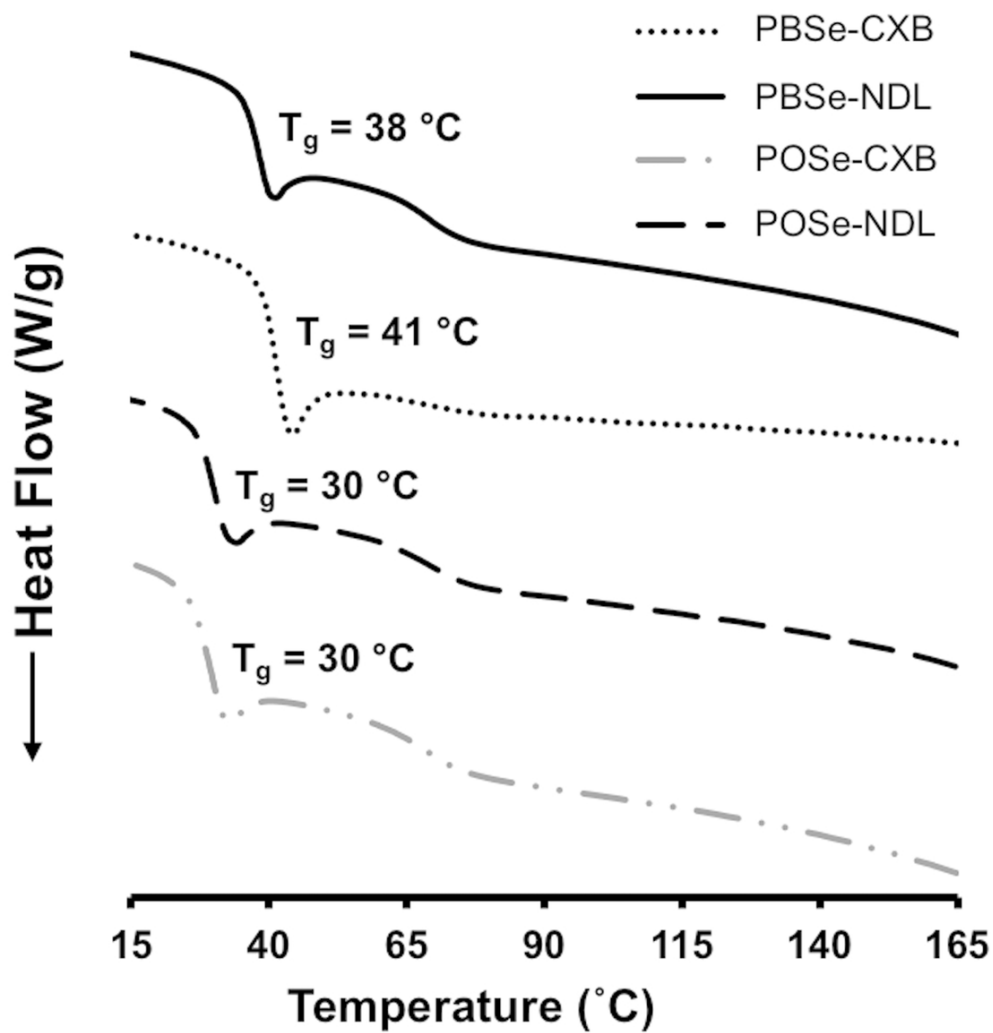


Figure 3. DSC thermograms of the drug-loaded and non-drug-loaded particles showing that the T_g was increased through CXB incorporation only for PBSe. A subtle transition corresponding to PVA was observed at 60 – 70 C but no melting temperature was observed for CXB.

94x100mm (300 x 300 DPI)

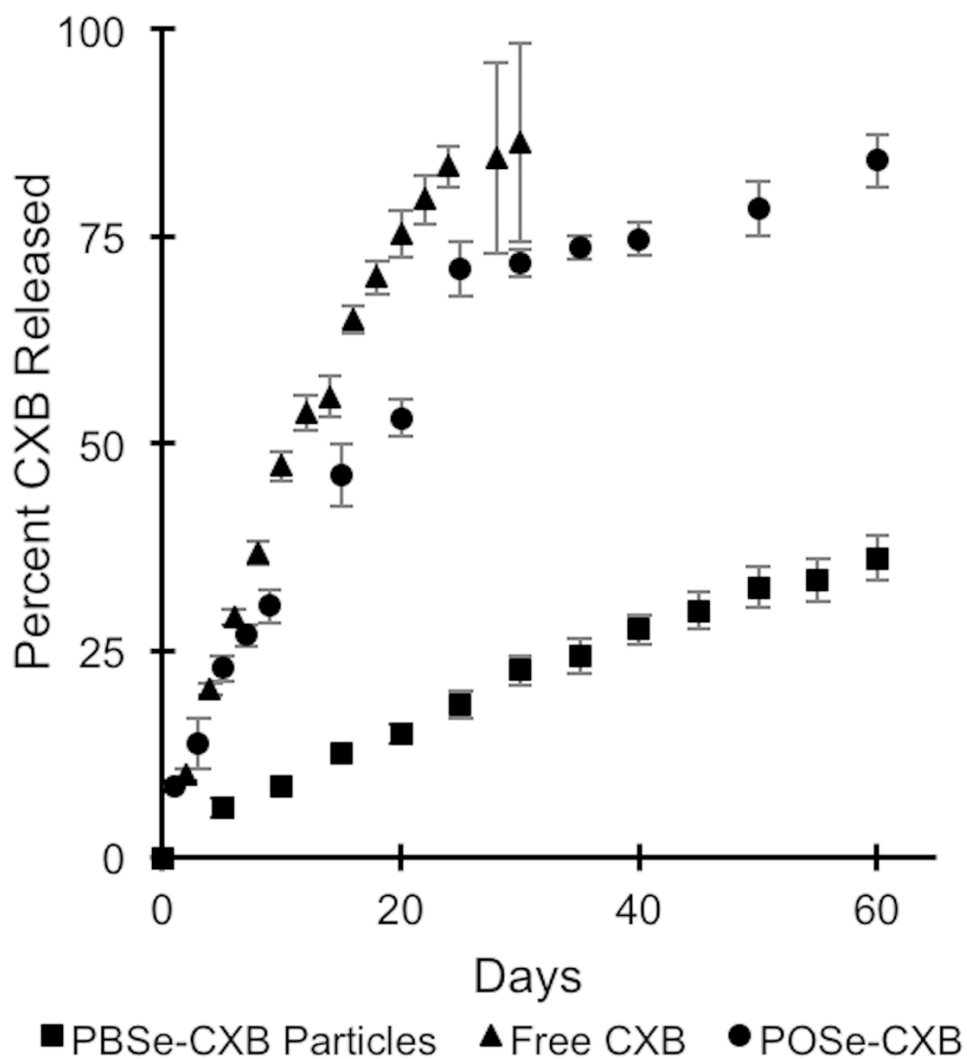


Figure 4. CXB release from PBSe-CXB particles and POSe-CXB particles in pH 7.4 PBS containing 2 wt% Tween 20 showing slower release of CXB from the PBSe-CXB particles. The release of insoluble free CXB through the dialysis membrane was also measured as a control to show that the release rate was not limited by the drug dissolution rate.

97x107mm (300 x 300 DPI)

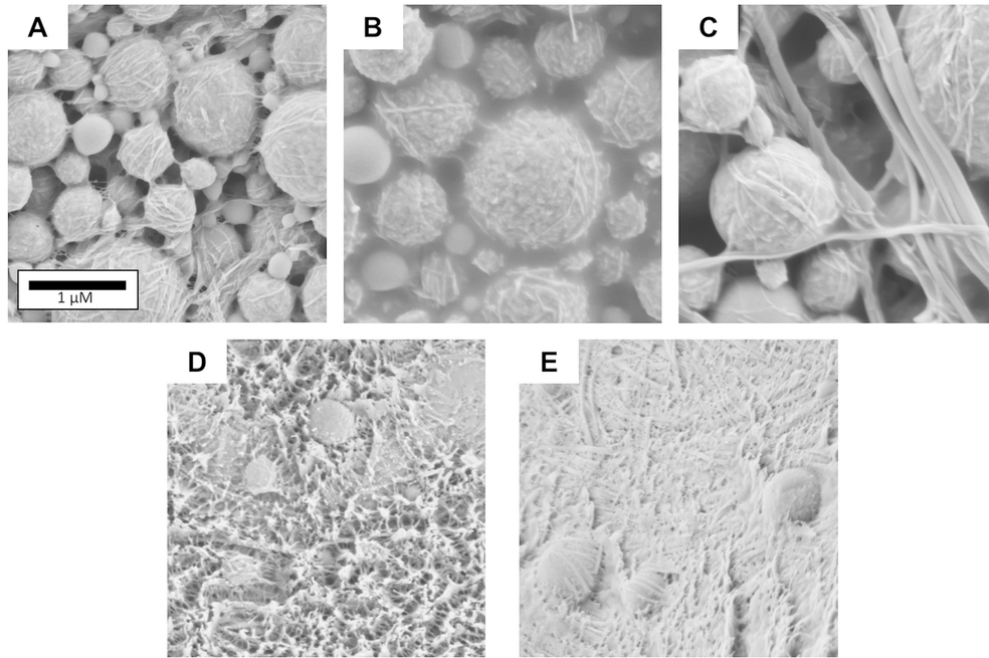


Figure 5. Degradation of PEA particles in pH 7.4 PBS at 37°C: A-C) PBSe-CXB particles after A) 14, B) 30 and C) 60 days; D-E) POSe-CXB particles after D) 7 and E) 14 days. All images were obtained at the same magnification. While particles were still observed for PBSe-CXB at 60 days, most of the POSe-CXB particles were rapidly eroded.

84x55mm (300 x 300 DPI)

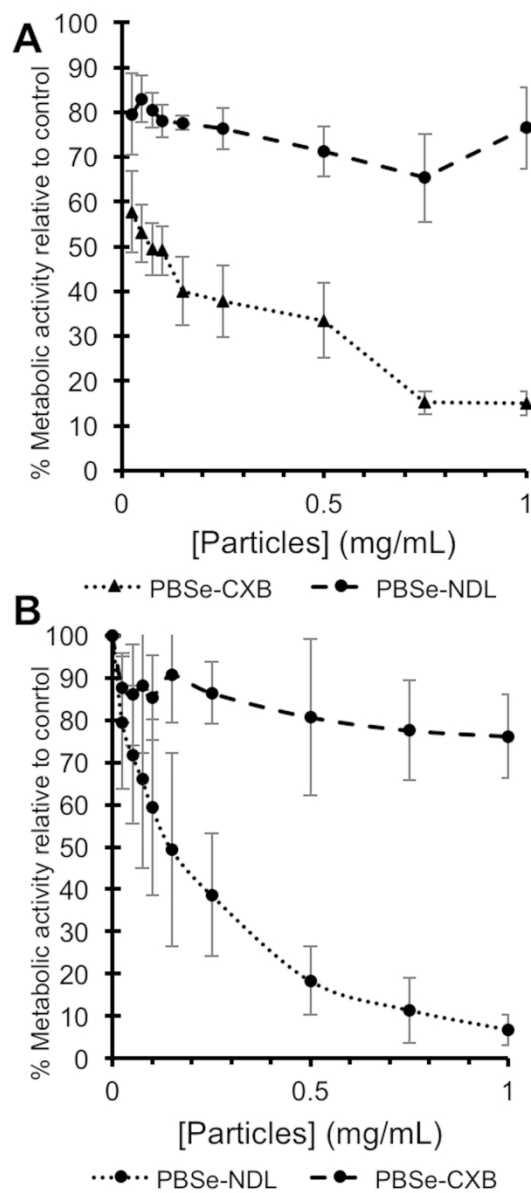


Figure 6. Metabolic activity of A) ATDC5 cells and B) C2C12 cells as measured by an MTT assay after a 48 h incubation with PBSe-CXB or PBSe-NDL particles (N = 4).

197x438mm (300 x 300 DPI)

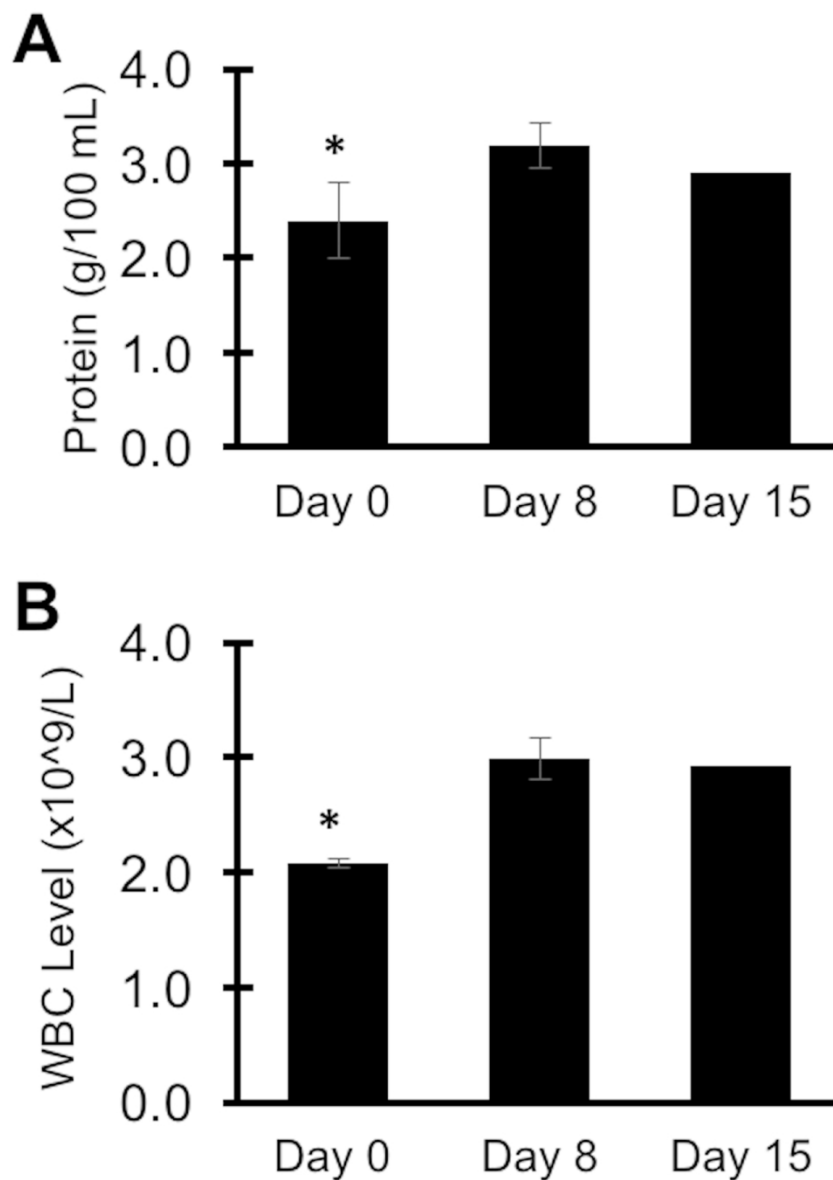


Figure 7. Synovial fluid analysis of injected sheep joints: A) Protein levels in synovial fluid at days 0, 8 and 15. * Indicates a significant difference between day 0 and day 8. (ANOVA $p = 0.04$) B) WBC levels at days 0, 8 and 15. * Indicates a statistically significant difference between day 0 and day 8 (ANOVA $p = 0.0001$). $N = 4$ at days 0 and 8 and $N = 2$ at day 15.

112x155mm (300 x 300 DPI)

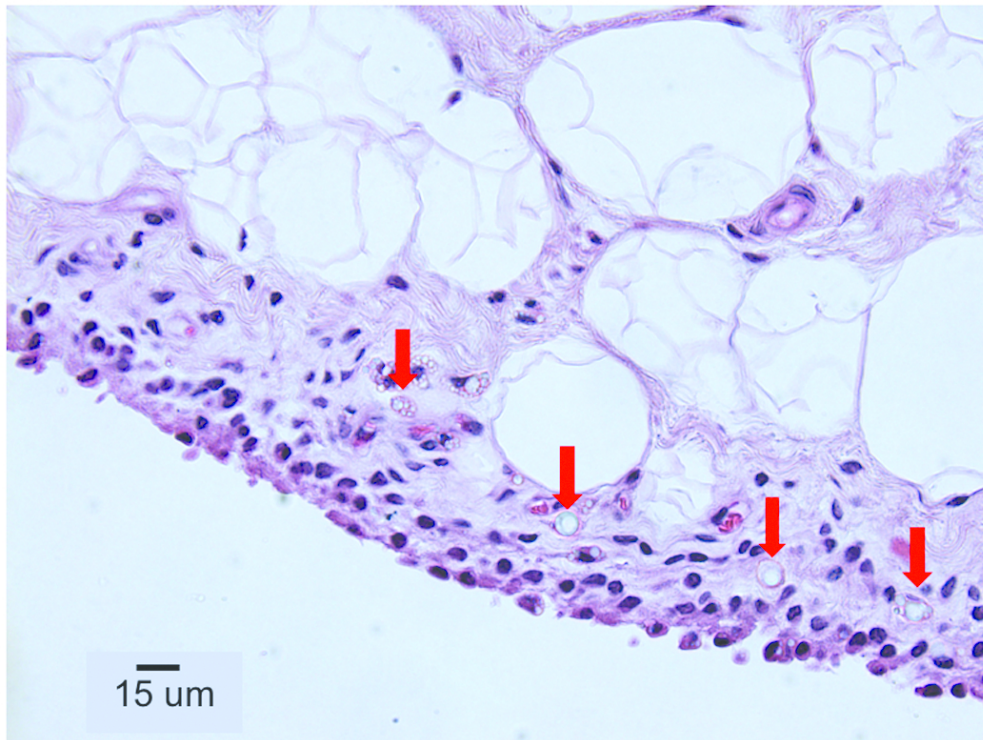


Figure 8. Immunohistochemical analysis of the synovial membrane of an injected sheep 15 days post injection. Hematoxylin and eosin staining was performed on sections of sheep synovium. Particles are visible within the membrane (indicated with red arrows).